Published in final edited form as:
J Am Chem Soc. 2010 December 22; 132(50): 17751–17759. doi:10.1021/ja104496q.

Accumulation of Tetrahedral Intermediates in Cholinesterase Catalysis: A Secondary Isotope Effect Study

Jose R. Tormos[1,2], **Kenneth L. Wiley**[1,3], **Yi Wang**[1,4], **Didier Fournier**[5], **Patrick Masson**[6], **Florian Nachon**[6], and **Daniel M. Quinn**[1,*]

[1]The University of Iowa, Department of Chemistry, Iowa City, Iowa 52242

[5]Différenciation Cellulaire et Croissance, INRA, 2 place Viala, 34060, Montpellier, France

[6]Centre de Recherches du Service de Santé Armées, Unité d'Enzymologie, BP 87-38702 La Tronche CEDEX, France

Abstract

In a previous communication, kinetic β-deuterium secondary isotope effects were reported that support a mechanism for substrate-activated turnover of acetylthiocholine by human butyrylcholinesterase (BuChE) wherein the accumulating reactant state is a tetrahedral intermediate (Tormos, J. R., *et al*. (2005) *JACS* **127**, 14538–14539). In this paper additional isotope effect experiments are described with acetyl-labeled acetylthiocholines ($CL_3COSCH_2CH_2N^+Me_3$; L = H or D) that also support accumulation of the tetrahedral intermediate in *Drosophila melanogaster* acetylcholinesterase (DmAChE) catalysis. In contrast to the aforementioned BuChE-catalyzed reaction, for this reaction the dependence of initial rates on substrate concentration is marked by pronounced substrate inhibition at high substrate concentrations. Moreover, kinetic β -deuterium secondary isotope effects for turnover of acetylthiocholine depended on substrate concentration, and gave the following: $^{D3}k_{cat}/K_m = 0.95 \pm 0.03$, $^{D3}k_{cat} = 1.12 \pm 0.02$ and ^{D3} β $k_{cat} = 0.97 \pm 0.04$. The inverse isotope effect on k_{cat}/K_m is consistent with conversion of the sp^2 hybridized substrate carbonyl in the E + A reactant state into a quasi-tetrahedral transition state in the acylation stage of catalysis, whereas the markedly normal isotope effect on k_{cat} is consistent with hybridization change from sp^3 toward sp^2 as the reactant state for deacylation is converted into the subsequent transition state. Transition states for *Drosophila melanogaster* AChE-catalyzed hydrolysis of acetylthiocholine were further characterized by measuring solvent isotope effects and determining proton inventories. These experiments indicated that the transition state for rate-determining decomposition of the tetrahedral intermediate is stabilized by multiple protonic interactions. Finally, a simple model is proposed for the contribution that tetrahedral intermediate stabilization provides to the catalytic power of acetylcholinesterase.

Keywords

Cholinesterase catalysis; catalytic power; secondary isotope effects; tetrahedral intermediate stabilization; transition state structure

[*]To whom correspondence should be addressed: Department of Chemistry, The University of Iowa, 315 CB, Iowa City, IA 52242; daniel-quinn@uiowa.edu; 319-335-1335.
[2]Current address: Department of Biochemistry, University of Texas Health Science Center, San Antonio, TX 78229, USA
[3]Current address: FDA National Center for Toxicological Research, 3900 NCTR Road, Jefferson, AR 72079, USA
[4]Current address: Medicinal Chemistry Department, 30 Corporate Circle, Albany, NY 12212, USA

Introduction

Enzymes of the cholinesterase family, and in particular acetylcholinesterase (AChE1), are noted for their very high catalytic activities, as illustrated by k_{cat}/K_m values of ~ 10^8 M^{-1} s^{-1} and k_{cat} values ~ 10^4 s^{-1}.2 The k_{cat} values exceed the rate constant for spontaneous, nonenzymic hydrolysis of acetylcholine (ACh) by 13–14 orders of magnitude,3 which corresponds to 74–79 kJ mol^{-1} of transition state stabilization. Illuminating the mechanistic features that give rise to this impressive catalytic power is of considerable importance, not only for the understanding of enzyme function thereby promoted, but also because the design of potent enzyme inhibitors of putative therapeutic potential is informed.

Report of the first crystal structure of butyrylcholinesterase (BuChE) by Nicolet *et al*.4 in 2003 provided a seminal structural view of a complex that accords with the catalytic power of cholinesterases. These authors found electron density near the nucleophilic oxygen of Ser198 in the active site that they interpreted as a covalently bound butyrate moiety; i.e., the bound ligand was a tetrahedral adduct of Ser198 and the butyrate carbonyl carbon that is, *pro forma*, the tetrahedral intermediate in the deacylation stage of catalysis. A subsequent kinetic β-deuterium isotope effect study of human BuChE-catalyzed hydrolysis of acetylthiocholine (ATCh) supported the crystallographic observations.5 This enzyme shows substrate activation at high substrate concentration, and the isotope effect on k_{cat} for the substrate-activated reaction = 1.29 ± 0.06, a value that is consistent with rate limiting decomposition of an accumulating tetrahedral intermediate in the deacylation stage of catalysis. On the other hand, the isotope effect on k_{cat} of the reaction absent substrate activation was within experimental error of unity. Consequently, a further implication of this finding is that the binding of a second molecule of acetylthiocholine at the substrate-activation site of the BuChE-substrate complex allosterically modulates the function of the active site.

In this paper kinetic β-deuterium isotope effects are applied to a second cholinesterase reaction, that of *Drosophila melanogaster* AChE (DmAChE) catalyzed hydrolysis of acetylthiocholine. In contrast to BuChE, and consistent with persistent observations for AChE,6 this enzyme shows substrate inhibition at high substrate concentrations. As will be discussed below, isotope effects again indicate that the deacylation stage of catalysis is rate limited by decomposition of an accumulating tetrahedral intermediate. Additionally, solvent isotope effects were measured and the proton inventory of k_{cat} was conducted to characterize the nature of the protonic interactions that stabilize the transition state for tetrahedral intermediate decomposition.

Experimental

Materials

Reagents for enzyme kinetics and for the synthesis of the isotopic acetylthiocholines (acetyl-L_3-thiocholines, L = H or ^{2}H) and the synthesis of diethylumbelliferyl phosphate were purchased from the following sources: (dimethylamino)ethanethiol, dichloromethane, umbelliferone, diethyl chlorophosphate, chloroform-d (99.8% ^{2}H), triethylamine, methyl iodide, 99.9% deuterium oxide, bovine serum albumin (BSA), 5,5’-dithiobis(2-nitorobenzoic acid) (DTNB), and sodium phosphate, monobasic, Sigma-Aldrich Chemical Co., St. Louis, MO; diethyl ether, sodium sulfate, sodium chloride, sodium hydroxide, and sodium phosphate, dibasic, Fisher Scientific, Pittsburgh, PA; d_6 acetic anhydride, Cambridge Isotopes Laboratories, Inc., Andover, MA.

Recombinant *Drosophila melanogaster* AChE (DmAChE) was expressed and purified as previously described.7 Stock enzyme solutions were diluted in reaction buffer (see below)

that contained 1 mg/mL of BSA; BSA stabilizes *Dm*AChE activity, as indicated by linear initial rates (data not shown) in the DTNB-coupled ATCh assay described by Ellman *et al*.8

Synthesis of Isotopic Acetylthiocholine

Acetyl-$^2H_3$-thiocholine iodide was synthesized by a modification of the method reported by Malany *et. al.* 9 To a mixture of (dimethylamino)-ethanethiol (32.7 mmol) and triethylamine (39.5 mmol) in a round-bottom flask with stirring in an ice bath (at 0 °C), d_6-acetic anhydride (39.3 mmol) was added dropwise via syringe. The ice bath was removed and the mixture was left stirring at room temperature for 4 hours, after which the reaction was quenched with H_2O. The reaction mixture was extracted into diethyl ether, and the ether phase washed with H_2O. The organic phase was dried with Na_2SO_4, filtered and rotoevaporated to eliminate traces of unreacted starting material. After rotoevaporation, an oil was obtained that was dissolved in diethyl ether, and methyl iodide (48.0 mmol) was added dropwise via syringe at room temperature. The mixture was left stirring overnight. The resulting white solid precipitate was dissolved in diethyl ether, filtered, and air-dried to give the final product acetyl-$^2H_3$-thiocholine iodide as a solid white powder in 64% yield: ^1H NMR (in ^2H_2O) δ 3.31 (s, 9H, $N(CH_3)_3$), 3.4 – 3.6 (m, 4H CH_2CH_2). No signal for acetyl-CH_3 was observed at 2.2 ppm, which establishes the isotopic purity as ≥ to 98%. Elemental analysis (FW = 292.20 for C_7H_{13} $^2H_3NOSI$): calculated C 28.77, H 5.52, N 4.79, O 5.48; determined C 28.70, H 5.57, N 4.83, O 5.61. Note that ^2H is detected as ^1H by the analytical methodology employed by Atlantic Microlab, Inc.

Synthesis of Diethylumbelliferyl Phosphate

Diethylumbelliferyl phosphate (DUMP) was synthezised by the following procedure. Umbelliferone (0.501 grams, 3.1 mmol) was dissolved in 5 mL of dichloromethane with stirring at room temperature. To this solution 0.3 g (3.0 mmol) of triethylamine was added. The mixture was stirred at room temperature for 1 hour. Then an equimolar amount of diethyl chlorophosphate (0.528 g, 3.1 mmol) was added dropwise via syringe, and the reaction was left stirring at room temperature overnight. The reaction was diluted with diethyl ether and the mixture washed with H_2O. The organic phase was then dried with Na_2SO_4. The ether was rotoevaporated and a crude yellow oil was obtained. The oil was further purified by silica gel chromatography, with ethyl acetate as the mobile phase. The isolated product was obtained as a white solid in a 52 % yield: ^{31}P NMR ($CDCl_3$, relative to external H_3PO_4) δ -6.42 (s, P); ^1H NMR ($CDCl_3$, relative to internal TMS) δ 1.32 (t, 6H, 2 CH_3), δ 4.20 (d, 4H, 2 CH_2), δ 6.31 (d, 1H, vinyl proton), δ 7.14 (m, 2H, aromatic protons), δ 7.43 and 7.63 (d, 1H, aromatic and vinyl protons).

Characterization of Synthetic Products

Acetyl-$^2H_3$-thiocholine and DUMP were characterized by NMR spectroscopy on a Bruker Avance Ultrashield DPX-300 Top Spin spectrometer. Spectra were processed with XWINMR version 3.5 software for determination of chemical shifts and integrated intensities. Elemental analyses were determined by Atlantic Microlab, Inc., Norcross, GA.

Titration of Enzyme Active Sites

Diethylumbelliferyl phosphate (DUMP) was used as a titrant to determine the concentration of the active sites of *Dm*AChE. As with other organophosphates, DUMP phosphorylates the active site serine of the enzyme irreversibly and stoichiometrically.10 A 6.9 mM stock solution of ATCh was prepared in 0.1 M NaH_2PO_4/Na_2HPO_4 buffer, pH = 7.57, was frozen prior to use, and thawed and kept on ice during kinetics experiments. A 0.5 μM stock solution of DUMP was prepared in acetonitrile, and 8 μL of this inhibitor solution were added to a glass vial that contained 200 μL of the enzyme in reaction buffer (see below).

Time-dependent inhibition of the enzyme was followed at 412 nm and 27.0 °C by measuring initial rates of ATCh hydrolysis as a function of time after addition of the inhibitor to the enzyme. Assays contained, in a total volume of 1.00 mL, 961 μL of reaction buffer (see below), 34 μL of ATCh stock solution, and 5 μL of the incubated enzyme-inhibitor mixture. Hence, the assays contained 0.23 mM ATCh and 0.02% acetonitrile (v/v). A control reaction was performed in which 8 μL of acetonitrile was added to 200 μL of buffered enzyme and initial rates were measured as above; this control reaction accounts for changes of enzyme activity that do not arise from the presence of the inhibitor DUMP.

Enzyme Kinetics and Data Analysis

Initial rates of AChE-catalyzed hydrolysis of ATCh were followed by the Ellman assay8 in a reaction buffer that contained 0.5 mM 5,5-dithiobis(2-nitrobenzoic acid) (DTNB) and 0.1 M Na_2HPO_4/NaH_2PO_4 (pH 7.57). Reactions were followed at 412 nm and 27 °C on the 96-well SPECTRAmax Plus 384 microplate reading UV-visible spectrophotometer. Background reaction rates were followed under the same conditions in reaction buffer in the absence of enzyme, and the net rates in the presence of enzyme were corrected by subtracting the corresponding background rates. Least-squares analyses and graphical presentation of data were performed by using SigmaPlot 8.0 (Systat, Chicago, IL).

Solvent Isotope Effects and Proton Inventory

Solvent isotope effects for AChE-catalyzed hydrolysis of ATCh were determined by measuring initial rates, as described in the preceding paragraph, in equivalent buffers of H_2O and D_2O. Equivalent buffers are those that contain the same concentrations of all solutes.11 Hence, a buffer equivalent to the pH 7.57 reaction buffer described above was prepared and its pD measured as 8.11.12 A proton inventory of V_{max} (and hence k_{cat}) was conducted by measuring initial rates in mixed isotopic buffers prepared from the equivalent H_2O and D_2O reaction buffers. Further details of the proton inventory experiment are described in the **Results** section.

Results

Concentration of Enzyme Active Sites

The concentration of active sites of DmAChE solutions was determined by a well precedented procedure.10 Accordingly, the enzyme was incubated with 20 nM DUMP, an irreversible inhibitor that phosphorylates Ser238 of the active site. Time progressive loss of enzyme activity was observed, such that at long reaction times 49 ± 6 % of the activity remained (data not schown). Dividing the concentration of DUMP by this fraction, and taking into account the dilution of the enzyme stock solution on addition of the inhibitor aliquot (see **Experimental**), gives an enzyme concentration of 42 ± 5 nM. This value is used to calculate DmAChE active site concentrations for the enzyme dilutions that were used in the various kinetics experiments described below.

Substrate Inhibition

Initial velocities of DmAChE-catalyzed hydrolysis of ATCh were acquired over a wide range of concentrations, as shown in Figure 1. At lower concentrations, the dependence of rate on substrate concentration follows Michaelis-Menten kinetics, but at higher concentrations deviation from this behavior is noted that is consistent with substrate inhibition. A general extension of the Michaelis-Menten formalism to include second-order substrate concentration effects that arise from substrate inhibition is shown in Scheme 1, from which is derived equation 1 for the dependence of initial velocity on substrate concentration. In the scheme and equation, K_A is the dissociation constant of the complexes

of ATCh and the peripheral site of DmAChE (see **Discussion**), and β is the fractional reduction of the value of k_{cat} that arises from turnover of the AEA complex. Least-squares fitting of the data in Figure 1 to equation 1 yields the following parameters: V_{max} = 46 ± 1 mA min^{-1} (mA = milliabsorbance) = 7.6 ± 0.2 × 10^{-4} *A* s^{-1}, K_m = 98 ± 9 μM, K_A = 18 ± 6 mM, β = 0.31 ± 07. Dividing the latter value of V_{max} by the absorptivity constant of the product, 12200 A M^{-1}, gives V_{max} = 6.3 ± 0.1 × 10^{-8} M s^{-1}. The value of the turnover number, calculated as $k_{cat} = V_{max}/[E]_T$, where $[E]_T$ = the concentration of DmAChE determined by active site titration (see **Experimental Section**), is k_{cat} = 1850 ± 50 s^{-1}.

$$V_i = \frac{V_{max}[A](1+\beta[A]/K_A)}{K_m(1+\beta[A]/K_A)+[A](1+[A]/K_A)} \quad (1)$$

Kinetic Isotope Effects

β-Deuterium secondary isotope effects on initial rates for DmAChE-catalyzed hydrolysis of ATCh were measured throughout the substrate concentration range of Figure 1, and are plotted in Figure 2. As the figure shows, the substrate isotope effects are very close to 1.00 at low substrate concentrations, rise to a normal isotope effect maximum in the range 1.10–1.15 at intermediate concentrations, and progressively decrease as substrate concentration is further increased into the concentration range where substrate inhibition is apparent in Figure 1. This seemingly complex dependence of the isotope effects on substrate concentration can be interpreted in terms of the mechanism of Scheme 2, which is an extension of the mechanism of Scheme 1 and that contains both microscopic rate constants for the acylenzyme mechanism of AChE catalysis2 and an accumulating tetrahedral intermediate in the deacylation stage of catalysis. Least-squares fitting of the dependence of the isotope effects on substrate concentration and associated interpretation thereof are discussed later.

Solvent Isotope Effects and Proton Inventory

In like manner to the results shown in Figure 1, the dependencies of initial velocities on substrate concentration were determined in equivalent buffers of H_2O and D_2O11 and are plotted in Figure 3. The corresponding least-squares fits to equation 1 give the following isotope effects on the kinetic and equilibrium parameters: $^{D2O}V_{max}$ = 2.06 ± 0.08, $^{D2O}K_m$ = 1.5 ± 0.2, $^{D2O}K_A$ = 1.1 ± 0.3, ^{D2O} β = 1.0 ± 0.2.

A proton inventory of $V_i \approx V_{max}$ was conducted by measuring initial velocities in equivalent buffers of H_2O and D_2O at an initial concentration of ATCh of 1.0 mM. This concentration was sufficient to give high fractional saturation of the enzyme – 95% in H_2O and 97% in D_2O – and hence a good approximation of V_{max}, but was low enough so that substrate inhibition was modest, *i.e.* only about 6% in each isotopic solvent. The general expression for the proton inventory when the solvent isotope effect arises from isotopic fractionation in the transition state is given by equation 2:11

$$V_{i,n} = V_{i,0}\prod_i(1 - n + n\varphi_i^T) \quad (2)$$

$V_{i,n}$ and $V_{i,0}$ are initial velocities of DmAChE-catalyzed hydrolysis of ATCh in mixed buffers of H_2O and D_2O of atom fraction of D = n and in H_2O, respectively, and ϕ_i^T are each of i fractionation factors that arise from transition state protonic interactions that contribute to the overall solvent isotope effect. Accordingly, the contribution of an individual transition state proton bridge, such as a proton transfer, to the isotope effect is $1/\phi_i^T$. It is usually possible with proton inventory data of reasonable precision to distinguish

proton transfer mechanisms that involve a single proton transfer (*i.e.* a linear dependence of $V_{i,n}$ on n) from those that involve two or more transition state proton bridges (*i.e.* polynomial dependencies of $V_{i,n}$ on n).11 Interpretation of the proton inventory is provided in the Discussion section.

Discussion

Origins and Interpretation of Secondary Isotope Effects

Kinetic β-secondary deuterium isotope effects provide a judicious probe of structural changes in the substrate that are mechanistic features of organic reactions,13 such as the AChE-catalyzed ester hydrolysis reactions described herein. For reactions that convert an sp^2-hybridized carbonyl carbon of the reactant state to sp^3 in the product, the equilibrium β-deuterium isotope effect will be inverse (*i.e.* < 1), and the corresponding kinetic isotope effect will more closely approximate the equilibrium isotope effect the more closely the transition state resembles the sp^3-hybridized product.9 Correspondingly, for reactions that convert sp^3-hybridized reactant states to sp^2-hybrized products, the kinetic and equilibrium β-secondary deuterium isotope effects will be normal (*i.e.* > 1).

For nonenzymic acyl transfer reactions, the most common mechanism is one in which the nucleophile attacks the susceptible carbonyl carbon of the substrate to form a high-energy, steady-state tetrahedral intermediate, whose decomposition yields the products.14 Since by the Hammond postulate15 the transition states for both steps of the mechanism will resemble the tetrahedral intermediate, hybridization of the susceptible carbonyl carbon will always change from sp^2 in the reactant state to sp^3 in the rate-limiting transition state, and the reaction will give an inverse kinetic β-secondary deuterium isotope effect.

As shown in Figures 1 and 3, DmAChE-catalyzed hydrolysis of ATCh is subject to substrate inhibition at high concentration. The functional topology of AChE gives rise to substrate inhibition. The active site of AChE sits at the bottom of a 2 nm deep gorge, and a second substrate binding site called the peripheral site at the opening of the gorge is the site of initial substrate binding to the enzyme on the pathway that leads to subsequent substrate diffusion down the gorge to the active site and catalytic turnover.16 Substrate inhibition arises when a second molecule of substrate binds at the peripheral site of AChE and prevents the release of products that resulted from turnover of an earlier-binding substrate molecule. Rosenberry and colleagues refer to inhibition of product release as steric blockade.17

The dependence of the kinetic β-secondary deuterium isotope effect on substrate concentration shows complex behavior. That is, $^{D3}V_i \sim 1.0$ at low substrate concentrations, a maximum is observed in the isotope effect of $^{D3}V_i = 1.10 – 1.15$ at intermediate concentrations, and a progressive decrease in the isotope effect at high substrate concentrations accompanies increasing substrate inhibition. These observations indicate that the observed isotope effects on initial rates respond to changes in the state of the enzyme as substrate concentration is increased, and the normal isotope effect maximum at intermediate substrate concentrations requires that the accumulating steady-state intermediate when the active site is saturated by substrate is a tetrahedral intermediate. To accommodate these features, the kinetic mechanism of Scheme 1 is elaborated in terms of microscopic rate constants in Scheme 2. The top line of the kinetic mechanism shows the pathway for substrate binding and subsequent turnover at lower substrate concentrations, where substrate inhibition is not prominent. In this case the measureable Michaelis-Menten rate constants are given by equations 3 and 4:

$$\frac{k_{cat}}{K_m}=\frac{k_1k_3}{k_2+k_3} \quad (3)$$

$$k_{cat}=\frac{k_3k_5k_7}{k_5k_7+k_3(k_5+k_6+k_7)} \quad (4)$$

At high substrate concentrations the bottom pathway in Scheme 2 is followed, substrate inhibition is observed, and, as implicated in Scheme 1 and equation 1, the asymptotic rate constant is that in equation 5:

$$\beta k_{cat}=\frac{k_3k_9k_{11}}{k_9k_{11}+k_3(k_9+k_{10}+k_{11})} \quad (5)$$

To determine the kinetic β-secondary isotope effects on the kinetic parameters, the ratio of isotopic versions of equation 1 is written, as in equation 6:

$${}^{D3}V_i={}^{D3}V_{max}\frac{1+\beta^{H3}[A]/K_A}{1+(\beta^{H3}/{}^{D3}\beta)[A]/K_A}\times\frac{(K_m^{H3}/{}^{D3}Km)(1+\beta^{H3}/{}^{D3}\beta)[A]/K_A)+[A](1+[A]/K_A)}{K_m^{H3}(1+\beta^{H3}[A]/K_A)+[A](1+[A]/K_A)} \quad (6)$$

The isotope effects on the parameters are ${}^{D3}V_{max} = V_{max}{}^{H3}/ V_{max}{}^{D3}$, ${}^{D3}K_m=K_m^{H3}/K_m^{D3}$, and ${}^{D3}\beta = \beta^{H3}/\beta{}^{D3}$, where the respective parameters for the isotopic substrates are denoted by following superscripts. Note that the isotope effect on V_{max}, *i.e.* ${}^{D3}V_{max}$, is also the isotope effect on k_{cat}, ${}^{D3}k_{cat} = k_{cat}{}^{H3}/k_{cat}{}^{D3}$, since $V_{max} = k_{cat}[E]^T$. An assumption is that there is no β-secondary deuterium isotope effect on K_A, the dissociation constant for binding of ATCh to the peripheral site of the enzyme. This is a reasonable assumption, since binding of ATCh to the peripheral site is weak, K_A = 18 mM (cf. Figure 1 legend), and does not involve chemical transformation of the substrate.

The kinetic β-deuterium secondary isotope effects on the initial velocities depend on substrate concentration, as shown in Figure 2. The data in the figure were fit to equation 6, with the values of K_A, K_m^{H3} and β^{H3} constrained at their values in the Figure 1 legend, and with ${}^{D3}V_{max}$, ${}^{D3}K_m$ and ${}^{D3}\beta$ as adjustable least-squares parameters. The fit in Figure 2 gives the following isotope effects: ${}^{D3}k_{cat}$ = 1.12 ± 0.01, ${}^{D3}K_m$ = 1.18 ± 0.04, and ${}^{D3}\beta$ = 0.87 ± 0.03. Additional isotope effects can be calculated from these values: ${}^{D3}k_{cat}/K_m$ = 0.95 ± 0.03 and ${}^{D3}\beta k_{cat} = {}^{D3}\beta{}^{D3}k_{cat}$ = 0.97 ± 0.04. As one can see from equation 3, k_{cat}/K_m contains rate constants for substrate binding to and release from the active site, k_1 and k_2, respectively, and for the chemical step(s) that convert the Michaelis complex EA to the acylenzyme intermediate (*i.e.* k_3). The observed isotope effect is inverse, which is consistent with conversion of the sp^2-hybridized carbonyl carbon of ATCh in the E + A reactant state to a quasi-tetrahedral transition state in the acylation stage of catalysis. In analogy to the common addition-elimination mechanism for nonenzymic acyl transfer reactions,14 one expects that nucleophilic attack by Ser238 of the active site on the carbonyl carbon of ATCh produces a tetrahedral intermediate that decomposes to the acylenzyme intermediate by expulsion of the thiocholine leaving group. The tetrahedral intermediate should proceed to the acylenzyme intermediate considerably more rapidly than it reverts to the Michaelis complex, since thiol is a better leaving group than alcohol. Consequently, the rate-limiting transition state for k_{cat}/K_m must be, at least in part, that for formation of the tetrahedral intermediate. This assignment is consistent with the observed inverse β-secondary deuterium

isotope effect. However, one does not know whether the observed isotope effect is intrinsic, or whether there is a commitment to catalysis18 that arises from partial rate limitation by the substrate binding k_1 step and that partially masks the intrinsic isotope effect. That is, the intrinsic isotope effect on k_3 may be yet more inverse than the observed $^{D3}k_{cat}/K_m$. Despite this limitation, the observed isotope effect does indicate a hybridization change from sp^2 in the reactant state to sp^3-like in the partially or solely rate limiting transition state for formation of the tetrahedral intermediate in the acylation stage of catalysis.

The markedly normal β-secondary deuterium isotope effect on k_{cat} stands in stark contrast to the isotope effect on k_{cat}/K_m. For DmAChE, k_{cat} is rate limited by events in the deacylation stage of catalysis.6 In Scheme 2, the deacylation stage of catalysis includes rate constants for formation of a tetrahedral intermediate and for its reversion to the acylenzyme intermediate, k_9 and k_{10}, respectively, and for decomposition of the tetrahedral intermediate to products, k_{11}. The normal isotope effect on k_{cat} requires that under conditions of substrate saturation of the active site the accumulating steady-state intermediate is one in which the carbonyl carbon of the substrate is sp^3 hybridized, and that the transition state for breakdown of this intermediate is one in which hybridization at the erstwhile tetrahedral carbonyl is more sp^2-like. Hence, the implication is that DmAChE has evolved.to stabilize the tetrahedral intermediate in the deacylation stage of catalysis to such an extent that it has become the reactant state for k_{cat}. This mechanistic assignment is supported by the markedly normal β-secondary deuterium isotope effect on the Michaelis constant, $^{D3}K_m = 1.18 \pm 0.04$. For a single substrate enzyme the general form for the Michaelis constant is $K_m = [E][A]/[EA]$. This does not mean, however, that K_m is the dissociation constant of the Michaelis complex. Rather, K_m relates free enzyme and substrate to all bound forms of enzyme along the reaction pathway in the steady-state. For the DmAChE-catalyzed hydrolysis of ATCh discussed herein, tetrahedral intermediate accumulation would be manifested by an isotope effect on K_m that is the equilibrium isotope effect for conversion of an sp^3-hybridized reactant to an sp^2-hybridized product, the free substrate and free enzyme. The magnitude of the isotope effect per D, $(1.18 \pm 0.04)^{1/3} = 1.06 \pm 0.01$, is consistent with this assignment.19

Solvent Isotope Effects and Proton Inventory

Secondary isotope effects described herein suggest that for k_{cat} decomposition of the tetrahedral intermediate in the deacylation stage of catalysis is cleanly rate limiting. Hence, a rare opportunity is realized for further characterization of a single step, and its associated transition state, in a complex, multi-step enzyme catalytic cascade. Accordingly, solvent isotope effects have been measured on the various kinetic parameters of DmAChE-catalyzed hydrolysis of ATCh by measuring the dependencies of initial rates on substrate concentration in matched buffers of H_2O and D_2O (cf. Figure 3). A sizeable isotope effect of modest uncertainty was measured on the maximal velocity, $^{D2O}V_{max} = 2.06 \pm 0.08$. In order to provide a model for the number of transition state proton bridges that give rise to this solvent isotope effect, a proton inventory was determined as the dependence of initial velocity on the atom fraction of D in the mixed H_2O/D_2O buffers. The proton inventory was conducted at a substrate concentration where $V_i \sim V_{max}$. As shown by the nonlinear fit in Figure 4, the proton inventory is well described by the following version of equation 2:

$$V_{i,n}=V_{i,0}\left(1-n+n\phi^T\right)^2 \quad (7)$$

The fit of the data in Figure 4 to this equation indicates that two transition state bridges make equal contributions to the solvent isotope effect of $1/\phi^T = 1.42 \pm 0.01$. A transition state model that accommodates these results is shown in Scheme 3. In this model, the transition state is stabilized by two proton bridges. One of the bridges is that for the proton

that is transferred from the imidazolium side chain of His480 to the leaving group (i.e. the γ-oxygen of Ser238) as the accumulated tetrahedral intermediate decomposes to the products. The second proton bridge likely arises from a putative “short, strong H-bond” between His480 and Glu367 (see references 20 and 21 for description and discussion of this short, strong H-bond), as Scheme 3 shows. These protonic interactions will generate inverse fractionation factors and associated contributions to the observed solvent isotope effect that are consistent with the quantitative analysis of the proton inventory of Figure 4.

An alternate though related interpretation of the proton inventory deserves attention. Kovach and collaborators measured the fractionation factor of the His-Glu proton bridge in BuChE20 and human AChE21 in inhibitor complexes that bear close structural resemblance to the tetrahedral intermediates of the catalytic cycle. For AChE, the complex with *m-N,N,N*-trimethylammoniotrifluoroacetophenone, an analog of the tetrahedral intermediate in the acylation stage of catalysis, had a fractionation factor $\phi = 0.76$, while covalent phosphonate and phosphate complexes, which are analogs of the tetrahedral intermediate in the deacylation stage of catalysis, had $\phi \approx 0.5$. Therefore, using $\phi^R = 0.6$ as a representative value for the isotopic fractionation factor of the tetrahedral intermediate reactant state, one writes the following equation for the proton inventory:

$$V_{i,n} = V_{i,0} \frac{(1 - n + n\phi^T)^z}{(1 - n + 0.6n)} \quad (8)$$

In equation 8 the least-squares adjustable variable z is the number of protons with fractionation factor ϕ^T that contribute to the solvent isotope effect. A fit that is indistinguishable from that shown in Figure 4 obtains when the proton inventory data are fit to equation 8. The parameters that result from the fit are $z = 3.3 \pm 0.6$ and $\phi^T = 0.69 \pm 0.05$. Therefore, each of three transition state proton bridges make contributions to the solvent isotope effect of $1/\phi^T = 1.4 \pm 0.1$. Whatever the model that one accepts, the salient feature of the respective analyses discussed herein is that AChE utilizes multiple proton bridges, which include proton transfers, to stabilize the transition state for decomposition of tetrahedral intermediates. Though it is not possible to parse the effect of proton bridges on transition state stabilization in detail, the prevailing attitude is that the contribution to catalytic power of the “short, strong H-bond” (see discussions in references 20 and 21) between Glu367 and His480 is modest, on the order of 1 – 2 kcal mol^{-1}.22,23 Hence, a judicious view is that this H-bond is a contributor, among a geometrically convergent array of interactions,24 that AChE effects to stabilize transition states of the chemical steps of its complex catalytic cascade.25

Contribution of Tetrahedral Intermediate Stabilization to Catalytic Power

Results discussed herein demonstrate that DmAChE stabilizes the tetrahedral intermediate in the deacylation stage of catalysis to such an extent that the intermediate accumulates during steady-state substrate turnover. The question then arises as to how much stabilization of tetrahedral intermediates might contribute to the catalytic acceleration that AChE effects. To address this question, the free energy profile for formation of the tetrahedral intermediate was constructed by taking the geometric sum of two parabolic functions, $\Delta G_R = kx^2$ and $\Delta G_{TI} = k(x-1)^2 + y$; *i.e.* $\Delta G^{-1} = \Delta G^{R\,-1} + \Delta G_{TI}^{\;-1}$, where ΔG_R and ΔG_{TI} are the free energy functions for the reactant and the tetrahedral intermediate, centered at fractional reaction progresses 0 and 1, respectively. The minimum of the reactant free energy function was set at 0 and the curvature k of both free energy functions and the vertical offset y of the minimum of the free energy function for the tetrahedral intermediate were adjusted empirically until the overall profile matched the free energy of activation for nonenzymic,

neutral hydrolysis of ACh3 and the endoergocity for formation of the tetrahedral intermediate of the nonenzymic reaction,26 as outlined in the next paragraph.

The free energy of activation was calculated according to transition state theory27 as follows:

$$\Delta G^{\ddagger}=RT\left(\ln\frac{kT}{h}-\ln(k_{uncat})\right) \quad (9)$$

In equation 9 *k* and h are Boltzmann's and Planck's constants, respectively, R is the gas constant, and $k_{uncat} = 8 \times 10^{-10}$ s^{-1} is Schowen's estimate of the rate constant for the neutral hydrolysis of ACh.3 Equation 9 gives $\Delta G^{\ddagger} = 30$ kcal mol^{-1} at T = 298 K. The estimate of Guthrie and Cullimore of the free energy of formation of the carbonyl hydrate of $MeCO_2Me$27 was used as a measure of the endoergocity of formation of the tetrahedral intermediate; *i.e.* $\Delta G^{o} = 11$ kcal mol^{-1}. These values were used to calibrate the free energy profile for the formation of the tetrahedral intermediate of the nonenzymic neutral hydrolysis of ACh, as outlined in the preceding paragraph and illustrated by the black curve in Figure 5. Then, in order to assess the effect of tetrahedral intermediate stabilization on transition state stabilization, and hence on catalytic power, the curvature k of the parabolic free energy functions that contribute to ΔG was held constant and the vertical offset y of the ΔG_{TI} function was set to zero, which results in the blue curve in Figure 5. Note that this procedure results in a free energy profile in which formation of the tetrahedral intermediate is isoergonic, *i.e.* $\Delta G^{o} = 0$, and therefore the tetrahedral intermediate has been stabilized by 11 kcal mol^{-1} and its free energy matches that of the reactant that precedes it. The specific stabilization of the tetrahedral intermediate in the AChE reaction leads to a decrease of the free energy of activation of 3.2 kcal mol^{-1}, which corresponds to a 220-fold acceleration of the AChE reaction over the nonenzymic reaction.

The rather modest contribution of tetrahedral intermediate stabilization to the 10^{13}-fold catalytic acceleration wrought by AChE arises from the fact that the activation free energy of the nonenzymic reaction is much greater than the endoergocity of formation of the tetrahedral intermediate. Because of this the fractional reaction progress at the transition state is close to 0.54 and the transition state is remote from the tetrahedral intermediate both in structure and in energy. When the tetrahedral intermediate is stabilized, the transition state shifts to a fractional progress of 0.50, and the modest associated structural rearrangement is manifested as a modest energetic stabilization of the transition state.

An alternate model for the tetrahedral intermediate in nonenzymic neutral hydrolysis of acetylcholine is that which comes from the computational study of Fuxreiter and Warshel of the catalytic acceleration that AChE effects.25 For the formation of the tetrahedral intermediate they calculate $\Delta G^{\ddagger} = 36$ kcal mol^{-1} and $\Delta G^{o} = 26$ kcal mol^{-1}. Their computed free energy of activation is reasonably close to the value of 30 kcal mol^{-1} that is used for the nonenzymic reaction in Figure 5. If one uses the proportion between their computed free energies to scale the value of ΔGo to an activation free energy of 30 kcal mol^{-1}, then $\Delta G^{o} =$ 21.7 kcal mol^{-1}. Using these free energy changes and repeating the analysis of Figure 5 gives a transition state stabilization of 6.7 kcal mol^{-1}, which corresponds to a catalytic acceleration of 8.2×10^{4}.

Why Do Tetrahedral Intermediates Accumulate in Cholinesterase Catalysis? Like the DMAChE reaction described herein, β-secondary deuterium isotope effects also support accumulation of tetrahedral intermediates in human BuChE5 and horse serum BuChE-catalyzed hydrolyses of ATCh.28 One therefore wonders what are the structural origins of

the observed tetrahedral intermediate (TI) stabilization. The x-ray structure of the complex of *Torpedo californica* AChE (TcAChE) and the transition state analog inhibitor *m-N,N,N*-trimethylammoniotrifluoroacetophenone (TMTFA)24 visualizes the interactions that are important determinants of TI stabilization. TMTFA is a very potent inhibitor of cholinesterases, with intrinsic K_i values of 15 fM, 4 fM, 1.3 fM and 2.4 fM for respective inhibitions of AChEs from *Torpedo californica*,29 mouse,30 *Electrophorus electricus*,29 and humans,31 and 1.5 pM for inhibition of equine serum BuChE. 20 In the crystal structure TMTFA is bound in a configuration that is a close structural mimic of the TI in the acylation stage of catalysis. There are four binding subsites that comprise the active site of AChE: a) the quaternary ammonium binding locus, that recognizes the N^+Me_3 moiety of TMTFA and substrates via cation-π, cation-anion, and cation-dipole interactions; b) the sterically circumscribed acyl binding site that confers on AChE preference for substrates with small acyl groups, such as acetyl; c) the catalytic triad, especially the γ-oxygen of the nucleophilic serine; d) the oxyanion hole, which interacts with the negatively charged hemiacetal oxygen of the bound TMTFA. These binding loci are arrayed in a tetrahedral geometry about the erstwhile carbonyl carbon of TMTFA in the complex. AChE, like other serine esterases, possesses a three-pronged oxyanion hole.32 In the TcAChE-TMTFA complex the oxyanion hole consists of the peptide NH moieties of Gly118, Gly119 and A201. This contrasts with the two-pronged oxyanion holes of the pancreatic serine proteases, which catalyze the hydrolysis of peptide bonds.33 The three-pronged oxyanion holes of cholinesterases should therefore be more effective in polarizing the carbonyl CO function of substrates and substrate-mimetic ligands and in concomitant stabilization of TIs. This view is supported by McCammon and coworkers, whose computational studies indicate that in the acylation stage of catalysis the oxyanion hole makes two H-bonds to the carbonyl oxygen of ACh in the Michaelis complex, but three H-bonds in the tetrahedral intermediate.34,35

Site-specific mutagenesis experiments suggest that Glu199 of TcAChE (Glu202 in mammalian AChE), a component of the quaternary ammonium binding locus of the active site,24 plays a role in specific stabilization of TIs. In the Glu202Gln mutants of human AChE and mouse AChE catalysis is modestly affected; i.e., k_{cat}/K_m is reduced only ~ 9-fold and ~ 7-fold, respectively.36,37 However, the effect on the affinity of mouse AChE for TMTFA is more pronounced, with a K_i increase of ~ 70-fold for the Glu202Gln mutant.37

Direct observation of structures that mimic tetrahedral intermediates in acyl transfer reactions of esters is rare but precedented. A classical example is provided by the crystal structure of the neurotoxin tetrodotoxin.38,39 A component of the structure is a hemiorthoester monoanion for tetrodoxin itself,38 or a hemiorthoester in the hydrobromide salt.39 The hemiorthoester and hemiorthester anion are models of tetrahedral intermediates in ester alcoholysis, and doubtless owe their stability to the preorganized intramolecular functional group array – ester carbonyl and alcohol nucleophile – that renders nucleophilic addition facile. Though attack of a water nucleophile on the acylenzyme intermediate in cholinesterase catalysis is not *pro forma* intramolecular, it is likely also to be facile due to the dense packing of functional groups in the active site.

Though the case for tetrahedral intermediate stability in cholinesterase function is of relatively recent origin, it is not without precedent in studies of serine hydrolase function. Stein conducted careful and thorough investigations of transition state structure and rate limitation for *Pseudomonas fluorescens* aryl acylamidase-catalyzed hydrolysis of p-nitroacetanilide.40 For k_{cat}/K_m, the β-secondary deuterium isotope effect was 0.83 ± 0.04. This value is, within error, the equilibrium isotope effect for tetrahedral intermediate formation in the acylation stage of catalysis. Interestingly, Stein estimated an isotope effect of 1.12 for the deacylation stage of catalysis, which is in essential agreement with the value for k_{cat} for DMAChE-catalyzed hydrolysis of ATCh reported herein. Stein interpreted his

normal isotope effect in terms of carbonyl polarization by the oxyanion hole and not as an indication of specific TI stabilization. However, the isotope effects for cholinesterase reactions5,28 and the crystallographic observation of a TI in the active site of human BuChE4 suggest that Stein's work was a harbinger of a more general phenomenon in the mechanisms of enzymes of the α/β-hydrolase family.

Conclusion

Secondary isotope effect data are presented herein that are consistent with the ability of *Drosophila melanogaster* AChE to stabilize tetrahedral intermediates to such an extent that they accumulate on the enzyme during substrate turnover under conditions of substrate saturation. This mechanistic model is supported by the observation of Nicolet *et al*.4 that a tetrahedrally distorted butyrate interacts covalently with the active site serine in the crystal structure of BuChE, and with the secondary isotope effect studies of Tormos et al.5 and Wiley et al.28 of BuChE-catalyzed hydrolysis of ATCh. Consequently, the case is building that cholinesterases defy the paradigm, taught in undergraduate organic chemistry courses, that most acyl transfer reactions transit high-energy, metastable tetrahedral adducts. A quantitative analysis suggests that specific stabilization of tetrahedral intermediates leads to a catalytic acceleration of 10^2 to 10^5. While important, this catalytic acceleration is modest in comparison to the 10^{13}-fold catalytic power manifested by cholinesterases. The salient conclusion, therefore, is that stabilization of transition states of the chemical steps of the mechanism is yet the decisive factor in the evolution of the catalytic power of enzymes of the cholinesterase family.25

Acknowledgments

KLW was a trainee of the Predoctoral Training Program in Biotechnology, NIH grant T32 GM008365.

References

1. Abbreviations: ACh, acetylcholine; AChE, acetylcholinesterase; ATCh, acetylthiocholine; BuChE, butyryl-cholinesterase; DmAChE, Drosophila melanogaster AChE; DTNB, 5,5-dithiobis(2-nitrobenzoic acid); DUMP, diethylumbelliferyl phosphate; TcAChE, Torpedo californica AChE; TI, tetrahedral intermediate; TMS, tetramethylsilane
2. a) Quinn DM. Chem. Rev. 1987; 87:955–979. b) Rosenberry TL. Adv. Enzymol. Relat. Areas Mol. Biol. 1975; 43:103–218. [PubMed: 891]
3. The catalytic acceleration effected by AChE is estimated by dividing $k_{cat} = 10^4\ s^{-1}$ by the rate constant for neutral hydrolysis of ACh, $k_{uncat} = 8 \times 10^{-10} s^{-1}$, estimated by Schowen: Schowen, RL. Transition States of Biochemical Processes. Gandour, RD.; Schowen, RL., editors. New York and London: Plenum Press; 1978. p. 85-88.
4. Nicolet Y, Lockridge O, Masson P, Fontecilla-Camps JC, Nachon F. J. Biol. Chem. 2003; 278:41141–41147. [PubMed: 12869558]
5. Tormos JR, Wiley KL, Seravalli J, Nachon F, Masson P, Nicolet Y, Quinn DM. J. Am. Chem. Soc. 2005; 127:14538–14539. [PubMed: 16231883]
6. Stojan J, Brochier L, Alies C, Colletier JP, Fournier D. Eur. J. Biochem. 2004; 271:1364–1371. [PubMed: 15030487]
7. a) Chaabihi H, Fournier D, Fedon Y, Bossy JP, Ravallec M, Devauchelle G, Cérutti M. Biochem. Biophys. Res. Commun. 1994; 203:734–742. [PubMed: 8074730] b) Estrada-Mondaca S, Fournier D. Prot. Expr. Purif. 1998; 12:166–172.
8. Ellman GL, Courtney KD, Andres V, Featherstone RM. Biochemical Pharmacology. 1961; 7:88–95. [PubMed: 13726518]
9. Malany S, Sawai M, Sikorski RS, Seravalli J, Quinn DM, Radić Z, Taylor P, Kronman C, Velan B, Shafferman A. J. Am. Chem. Soc. 2000; 122:2981–2987.
10. Levy D, Ashani Y. Biochem. Pharmacol. 1986; 35:1079–1085. [PubMed: 3754444]

11. Quinn, DM.; Sutton, LD. Enzyme Mechanism from Isotope Effects. Cook, PF., editor. Boca Raton, FL: CRC Press; 1991. p. 73-126.
12. The pD of an equivalent buffer in D2O is determined by adding 0.4 to the pH meter reading: Salomaa P, Schaleger LL, Long FA. J. Am. Chem. Soc. 1964; 86:1–7.
13. Hogg, JL. Transition State of Biochemical Processes. Gandour, RD.; Schowen, RL., editors. New York and London: Plenum Press; 1978. p. 201-224.
14. Isaacs, N. Physical Organic Chemistry. Harlow, England: Addison Wesley Longman Ltd.; 1995. p. 507-536.
15. Hammond GS. J. Am. Chem. Soc. 1955; 77:334–338.
16. Sussman JL, Harel M, Frolow F, Oefner C, Goldman A, Toker L, Silman I. Science. 1991; 253:872–879. [PubMed: 1678899]
17. Szegletes T, Mallender WD, Thomas PJ, Rosenberry TL. Biochemistry. 1999; 38:122–133. [PubMed: 9890890]
18. Northrop, DB. Isotope Effects on Enzyme-Catalyzed Reactions. Cleland, WW.; O'Leary, MH.; Northrop, DB., editors. Baltimore, MD, USA: University Park Press; 1977. p. 122-150.
19. The 6% isotope effect per D for equilibrium decomposition of a tetrahedral intermediate compares favorably with the isotope effect in a model system, the equilibrium hydration of 1,3-dichloroacetone, for which $^{D4}K_{eq} = 0.83 \pm 0.04$ Hegazi, MF.; Quinn, DM.; Schowen, RL. Transition States of Biochemical Processes. Gandour, RD.; Schowen, RL., editors. New York and London: Plenum Press; 1978. p. 405-411. Therefore, in the dehydration direction the isotope effect is 1.20 ± 0.06, and the per D isotope effect is $(1.20 \pm 0.06)^{¼} = 4.8 \pm 1.2\%$.
20. Viragh C, Harris TK, Reddy PM, Massiah MA, Mildvan A, Kovach IM. Biochemistry. 2000; 39:16200–16205. [PubMed: 11123949]
21. Massiah MA, Viragh C, Reddy PM, Kovach IM, Johnson J, Rosenberry TL, Mildvan AS. Biochemistry. 2001; 40:5682–5690. [PubMed: 11341833]
22. QM-MM MD simulations of the mechanism of AChE-catalyzed hydrolysis of ACh suggest that the Glu-His H-bond in the catalytic triad is "…stronger than the normal hydrogen bond" by 1 – 2 kcal mol^{-1}. See: Zhou Y, Wang S, Zhang Y. J. Phys. Chem. B. 2010:8817–8825. [PubMed: 20550161]
23. Schowen has discussed the modest contributions to transition state stabilization of serine protease reactions that arises from the Asp-His H-bond of the active site triad, which functions in a manner that is analogous to that of the Glu-His H-bond in AChE catalysis. See: Schowen, RL. Isotope Effects in Chemistry and Biology. Kohen, A.; Limbach, H-H., editors. Boca Raton, FL, USA: CRC Press; 2006. p. 765-792.
24. Harel M, Quinn DM, Nair HK, Silman I, Sussman JL. J. Am. Chem. Soc. 1996; 118:2340–2346.
25. Fuxreiter M, Warshel A. J. Am. Chem. Soc. 1998; 120:183–194.
26. Guthrie JP, Cullimore PA. Can J. Chem. 1980; 58:1281–1294.
27. Glasstone, S.; Laidler, KJ.; Eyring, H. Theory of Rate Processes. New York and London: McGraw-Hill; 1941. p. 184-197.
28. Wiley KL, Tormos JR, Quinn DM. Chem.-Biol. Interact. 2010; 187:124–127. [PubMed: 20493178]
29. Nair HK, Seravalli J, Arbuckle T, Quinn DM. Biochemistry. 1994; 33:8566–8576. [PubMed: 8031791]
30. Quinn DM, Feaster SR, Nair HK, Baker NA, Radić Z, Taylor P. J. Am. Chem. Soc. 2000; 122:2975–2980.
31. Ordentlich A, Barak D, Kronman C, Ariel N, Segall Y, Velan B, Shafferman A. J. Biol. Chem. 1998; 273:19509–19517. [PubMed: 9677373]
32. Quinn, DM.; Medhekar, R.; Baker, NR. Enzymes, Enzyme Mechanisms, Proteins and Aspect of NO Chemistry. In: Poulter, CD., editor. Comprehensive Natural Product Chemistry. Vol. Vol. 3. Oxford, UK: Elsevier; 1999. p. 101-137.
33. Polgar, L. Hydrolytic Enzymes. Neuberger, A.; Brocklehurst, K., editors. Amsterdam: Elsevier; 1984. p. 159-200.

34. Zhang Y, Kua J, McCammon JA. J. Am. Chem. Soc. 2002; 124:10572–10577. [PubMed: 12197759]
35. Zhang Y, Kua J, McCammon JA. J. Phys. Chem. B. 2003; 107:4459–4463.
36. Malany S, Sawai M, Sikorski RS, Seravalli J, Quinn DM, Radić Z, Taylor P, Kronman C, Velan B, Shafferman A. J. Am. Chem. Soc. 2000; 122:2981–2987.
37. Radić Z, Kirchchoff PD, Quinn DM, McCammon JA, Taylor P. J. Biol. Chem. 1997; 272:23265–23277. [PubMed: 9287336]
38. Woodward RB, Gougoutas JZ. J. Am. Chem. Soc. 1964; 86:5030.
39. Furusaki A, Tomiie Y, Nitta I. Bull. Chem. Soc. Jap. 1970; 43:3332–3341.
40. Stein RL. Biochemistry. 2002; 41:991–1000. [PubMed: 11790123]

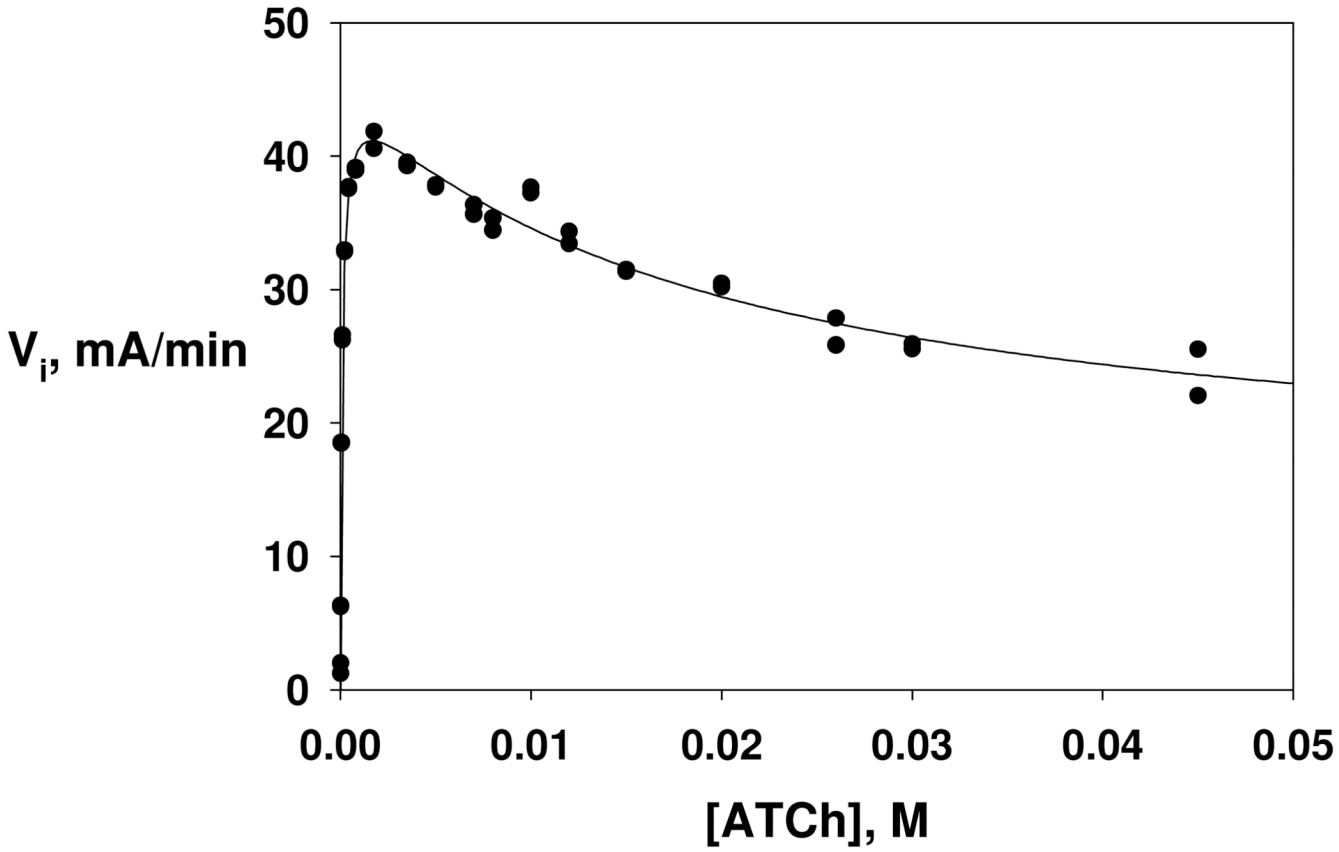

Figure 1.

Dependence of initial velocity on substrate concentration for DmAChE-catalyzed hydrolysis of ATCh. Reaction conditions and data acquisition are described in the **Experimental** section. The parameters of the least-squares fit to equation 1 of the text are $V_{max} = 46 \pm 1$ mA min^{-1} (mA = milliabsorbance), $K_m = 98 \pm 9$ μM, $K_A = 18 \pm 6$ mM, $\beta = 0.31 \pm 0.07$.

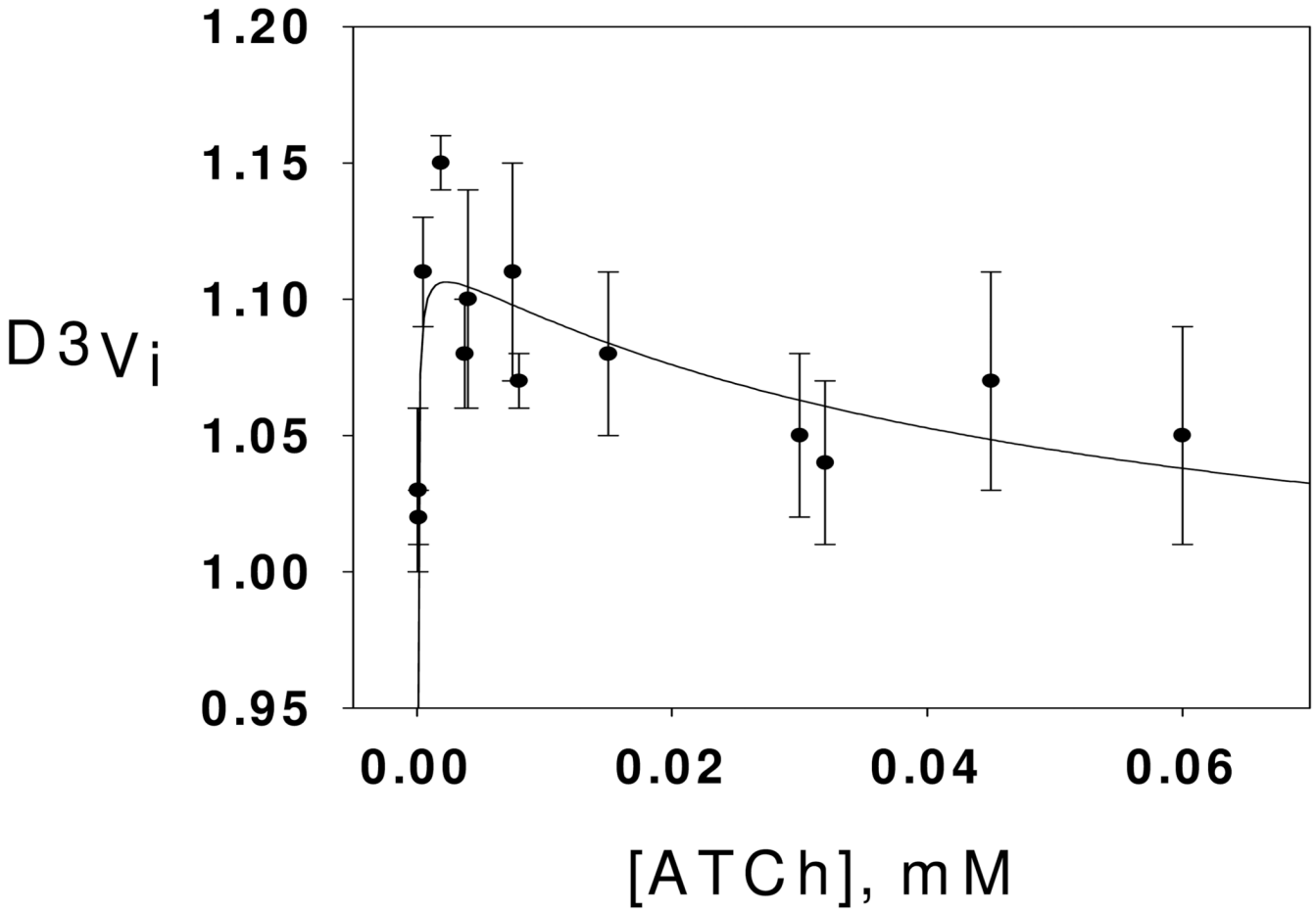

Figure 2.
Dependence β-deuterium secondary isotope effects on substrate concentration for DmAChE-catalyzed hydrolysis of ATCh. Reaction conditions and data acquisition are described in the **Experimental** section. The parameters of the least-squares fit to equation 2 (see text) are $^{D3}V_{max}$ = 1.12 ± 0.01, $^{D3}K_m$ = 1.18 ± 0.04, and $^{D3}\beta$= 0.87 ± 0.03.

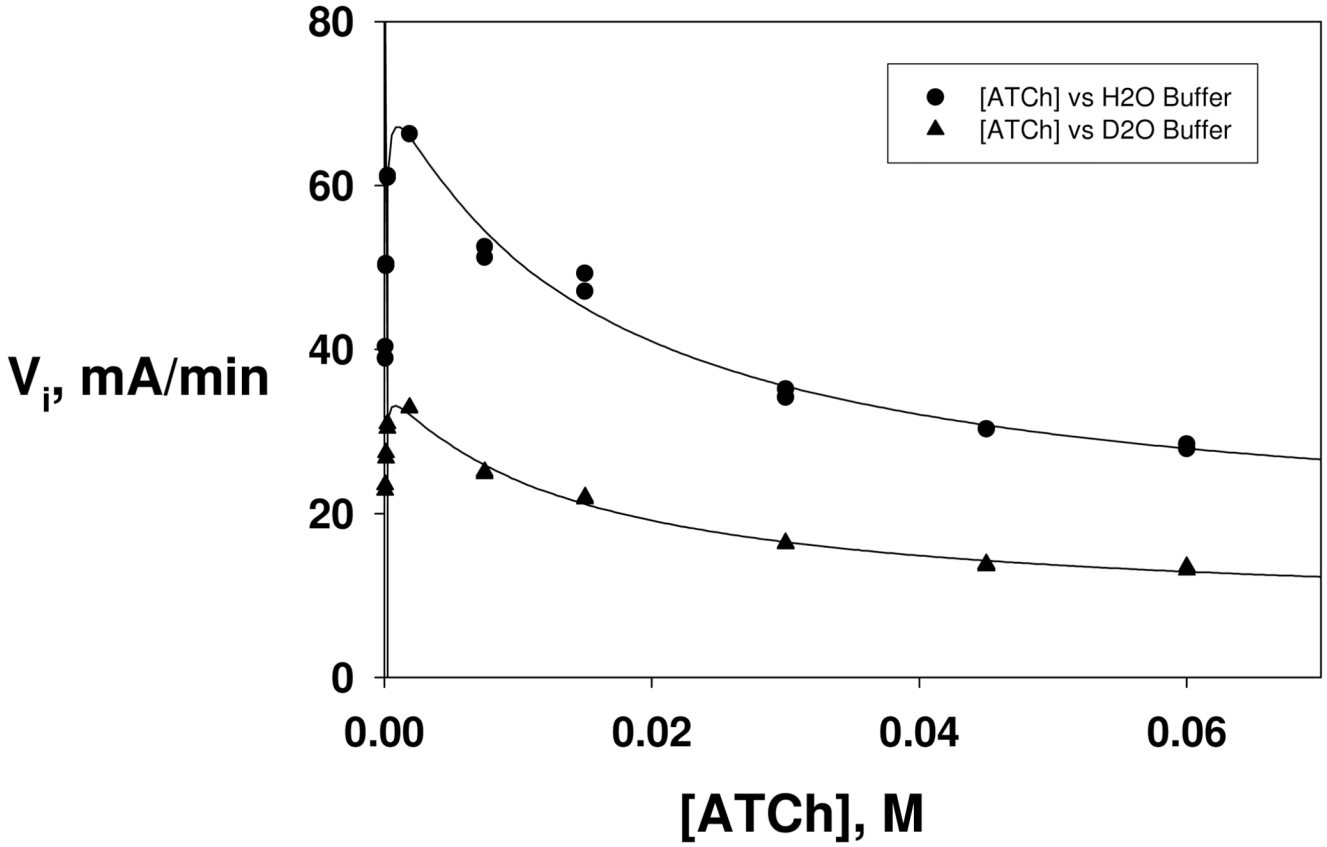

Figure 3.

Dependencies of initial velocities of DmAChE-catalyzed hydrolysis of ATCh on substrate concentration in equivalent buffers of H_2O (circles) and D_2O (triangles). Reaction conditions and data acquisition are described in the **Experimental** section. Each curve was fitted by least-squares to equation 1 of the text, and the following isotope effects were calculated from the least-squares parameters: $^{D2O}V_{max} = 2.06 \pm 0.08$, $^{D2O}K_m = 1.5 \pm 0.2$, $^{D2O}K_A = 1.1 \pm 0.3$, $^{D2O}\beta = 1.0 \pm 0.2$.

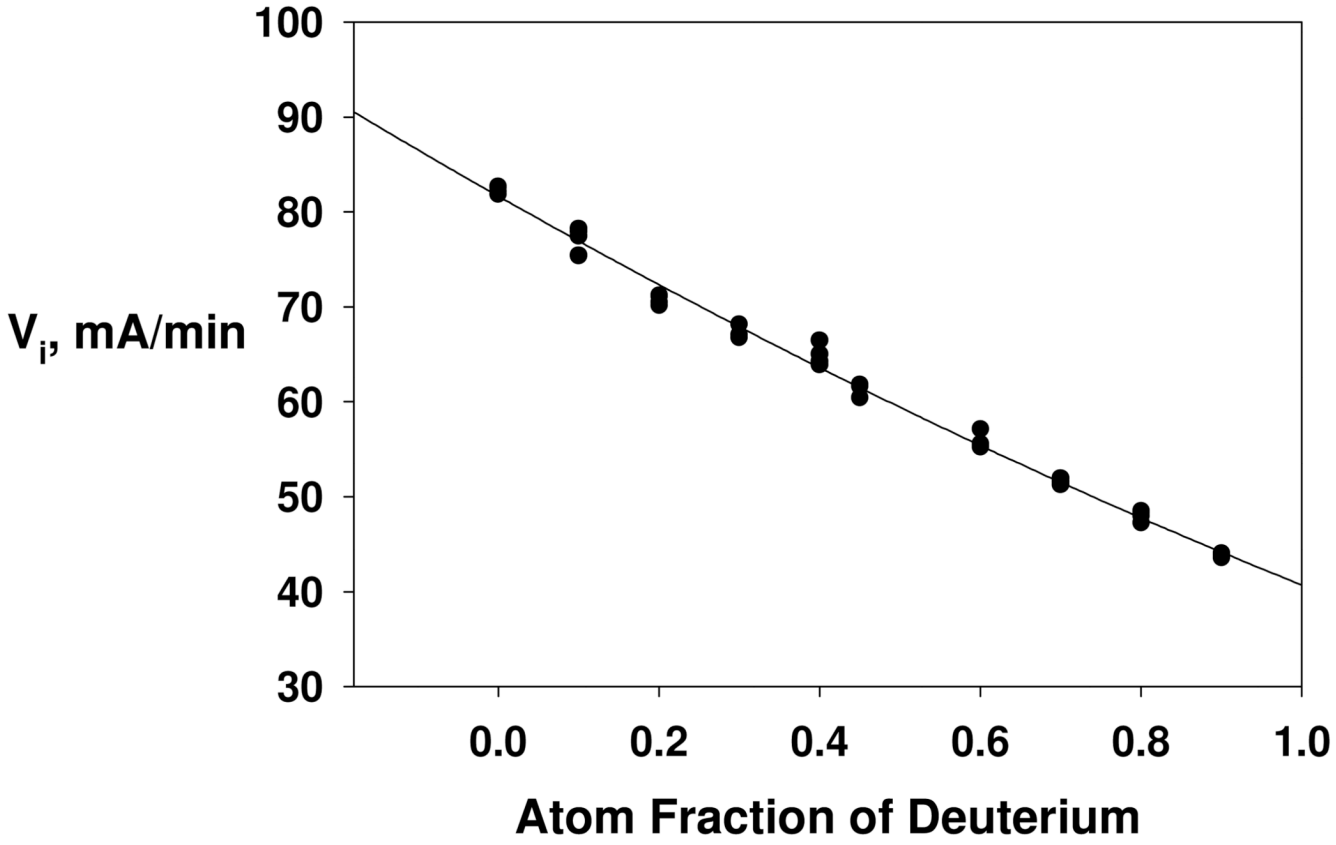

Figure 4.

Proton inventory of $V_i \approx V_{max}$ for DmAChE-catalyzed hydrolysis of ATCh. The initial substrate concentration was $[ATCh]_0$ = 1.0 mM = 20 K_m in buffered H_2O and 28 K_m in buffered D_2O. The curve is a least-squares fit of the data to equation 4 of the text, which ascribes the overall solvent isotope effect $^{D2O}V_i$ = 1.99 as arising from equal contributions of two transition state proton bridges, each generating an isotope effect of 1.41 (*i.e.* $\phi_1{}^T = \phi_2{}^T = 0.706 \pm 0.004$). Additional reaction conditions and data acquisition methods are described in the **Experimental** section.

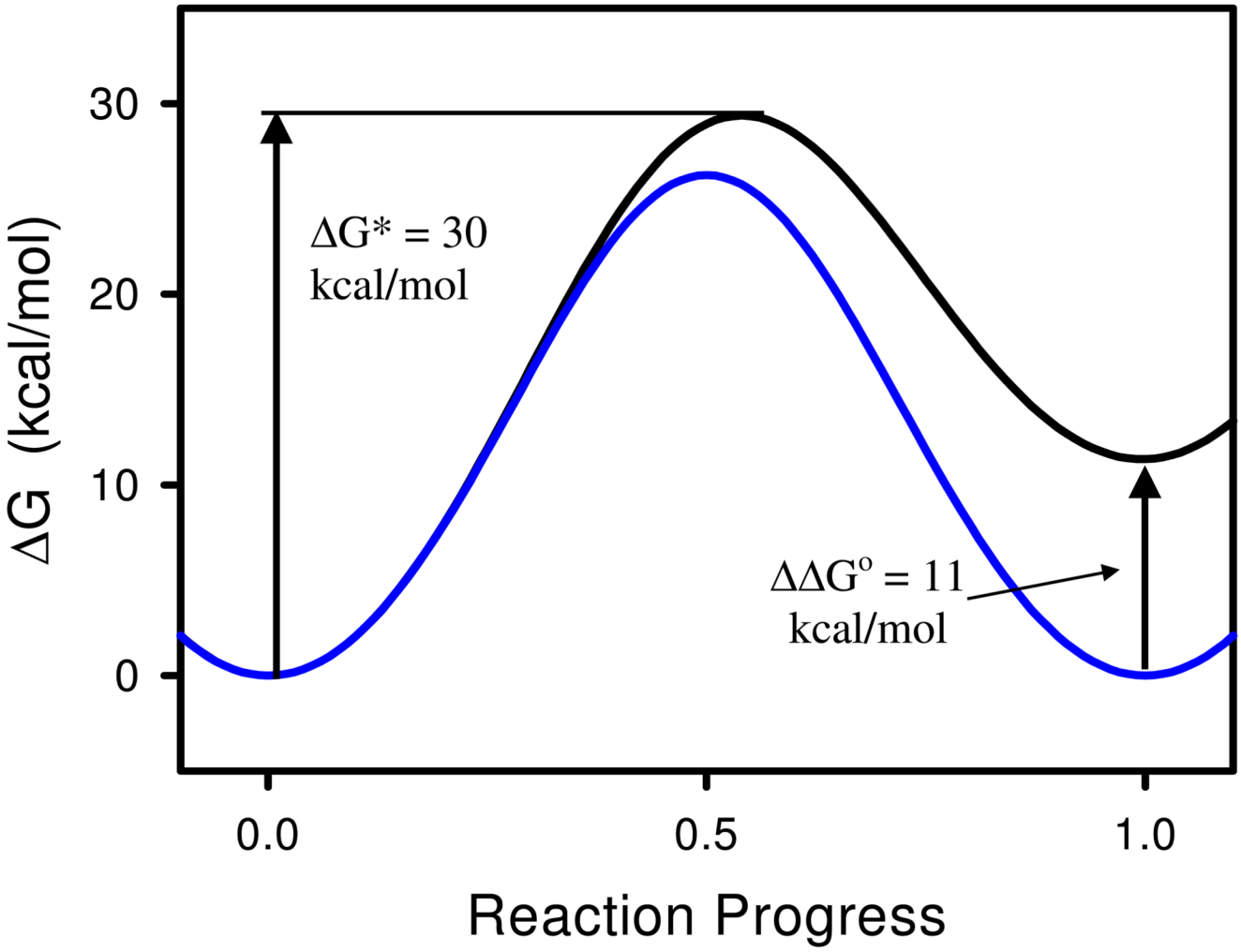

Figure 5.
Free energy profiles for formation of the tetrahedral intermediate in nonenzymic (black line) and AChE-catalyzed (blue line) hydrolysis of ACh. The sp^2-hybridized reactant is at fractional reaction progress 0, and the sp^3-hybridized tetrahedral intermediate is at fractional reaction progress 1. The free energy profile for the nonenzymic reaction was calibrated as described in the text. The profile for AChE catalysis was generated by stabilizing the tetrahedral intermediate by 11 kcal mol^{-1}, as also described in the text.

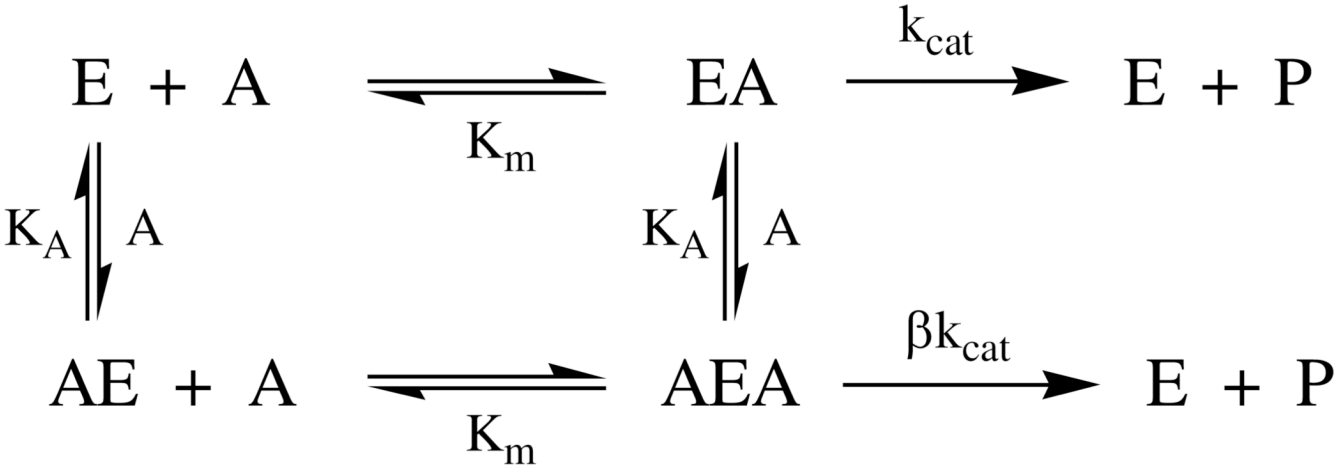

Scheme 1.

AChE kinetic mechanism that accounts for substrate inhibition at high substrate concentrations.

E = free enzyme

EA = Michaelis complex

A = substrate

P = product

AE = complex of substrate at peripheral site

K_m = Michaelis constant

AEA = Michaelis complex with substrate bound at peripheral site

k_{cat} = turnover number

β= residual kcat of AEA complex

K_A = dissociation constant for binding of substrate to the peripheral site in AE and AEA complexes

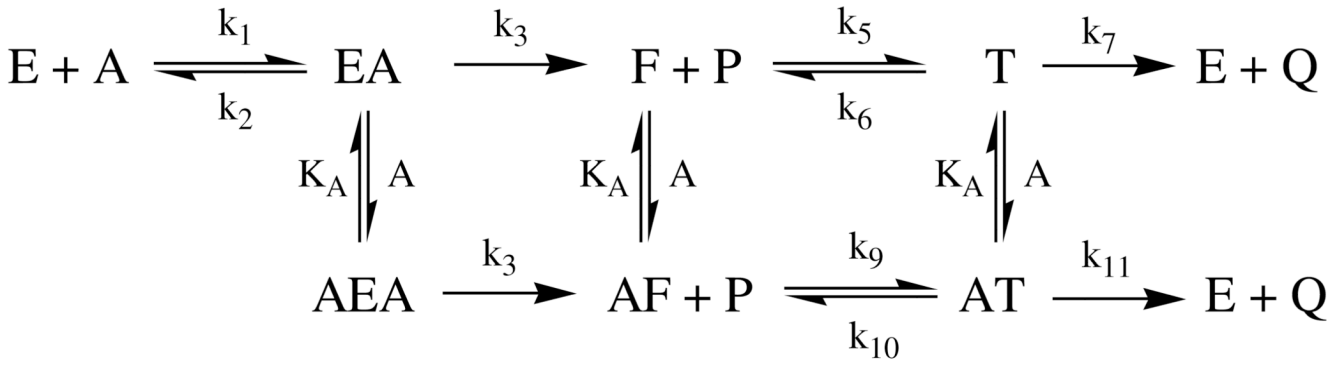

Scheme 2.

AChE kinetic mechanism that accommodates substrate inhibition and includes an accumulating tetrahedral intermediate in the deacylation stage of catalysis.

P = thiocholine product

Q = acetate product

F = acylenzyme intermediate

T = tetrahedral intermediate

AF = acylenzyme intermediate with substrate at peripheral site

AEA = Michaelis complex with substrate at peripheral site

AT = tetrahedral intermediate with substrate at peripheral site

K_A = dissociation constant of AEA, AF and AT complexes

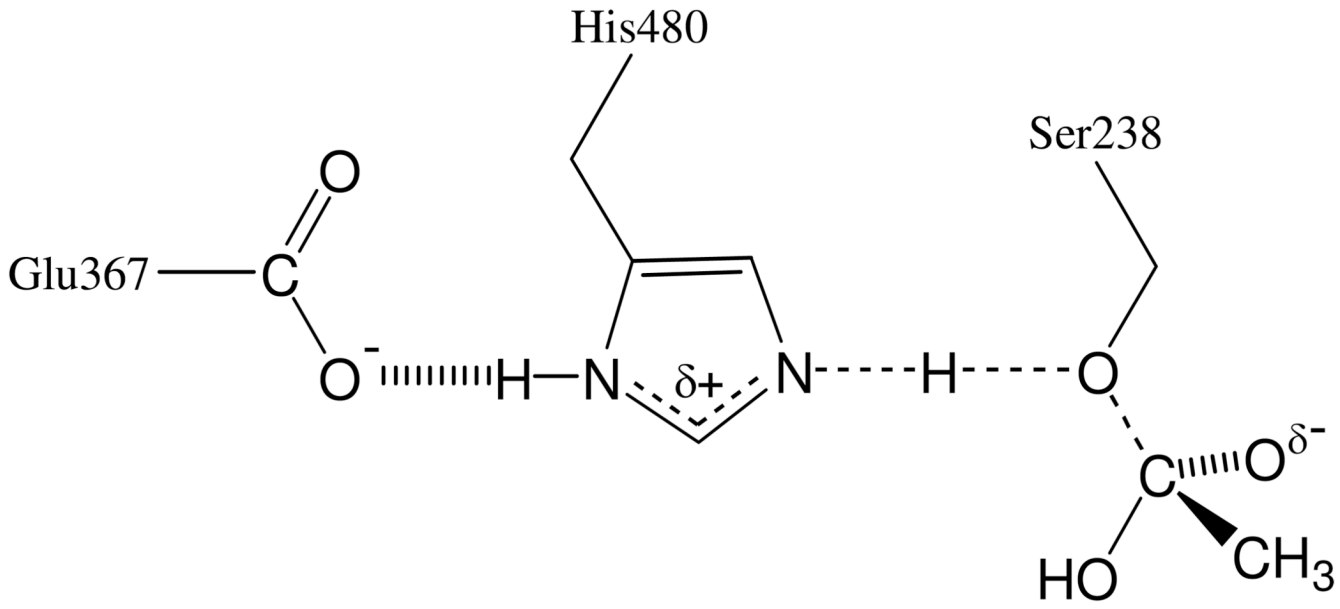

Scheme 3.
Protonic interactions and covalency changes in the transition state for rate-limiting decomposition of the tetrahedral intermediate in the deacylation stage of DmAChE catalysis.